ODE Transformer: An Ordinary Differential Equation-Inspired Model for Sequence Generation

Anonymous ACL submission

Abstract

Residual networks are an Euler discretization of solutions to Ordinary Differential Equations (ODE). This paper explores a deeper relationship between Transformer and numerical ODE methods. We first show that a residual block of layers in Transformer can be described as a higher-order solution to ODE. Inspired by this, we design a new architecture, *ODE Transformer*, which is analogous to the Runge-Kutta method that is well motivated in ODE. As a natural extension to Transformer, ODE Transformer is easy to implement and efficient to use. Experimental results on the large-scale machine translation, abstractive summarization, and grammar error correction tasks demonstrate the high genericity of ODE Transformer. It can gain large improvements in model performance over strong baselines (e.g., 30.77 and 44.11 BLEU scores on the WMT'14 English-German and English-French benchmarks) at a slight cost in inference efficiency.

1 Introduction

Residual networks have been used with a great success as a standard method of easing information flow in multi-layer neural models (He et al., 2016; Vaswani et al., 2017). Given an input y_t, models of this kind define the output of a layer t to be:

$$y_{t+1} = y_t + F(y_t, \theta_t) \quad (1)$$

where $F(\cdot, \cdot)$ is the function of the layer and θ_t is its parameter. Interestingly, recent work in machine learning (Weinan, 2017; Lu et al., 2018; Haber et al., 2018; Chang et al., 2018; Ruthotto and Haber, 2019) points out that Eq. (1) is an Euler discretization of the Ordinary Differential Equation (ODE), like this:

$$\frac{\mathrm{d}y(t)}{\mathrm{d}t} = F(y(t), \theta(t)) \quad (2)$$

where $y(t)$ and $\theta(t)$ are continuous with respect to t. In this way, we can call Eq. (1) an *ODE block*.

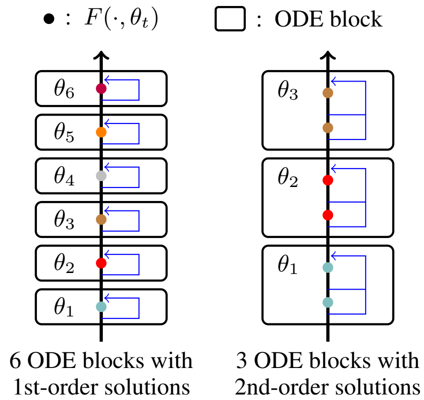

Figure 1: Models with different ODE blocks.

This finding offers a new way of explaining residual networks in the view of numerical algorithms. Then, one can think of a multi-layer network as applying the Euler method (i.e., Eq. (1)) to solve Eq. (2) subject to the initial conditions $y(0) = y_0$ and $\theta(0) = \theta_0$.

The solution of Eq. (2) has a sufficiently low error bound (call it a *stable solution*) only if $\theta(t)$ changes slow along t (Haber and Ruthotto, 2017; Chen et al., 2018). But this assumption does not always hold for state-of-the-art natural language processing (NLP) systems, in which models are non-linear and over-parameterized. For example, language modeling and machine translation systems learn quite different parameters for different layers, especially when the layers are close to the model input (Vaswani et al., 2017; Dai et al., 2019). Also, truncation errors are nonnegligible for the Euler method because it is a first-order approximation to the true solution (He et al., 2019). These problems make the situation worse, when more layers are stacked and errors are propagated through the neural network. It might explain why recent Machine Translation (MT) systems cannot benefit from extremely deep models (Wang et al., 2019; Liu et al., 2020a; Wei et al., 2020; Li et al., 2020).

This paper continues the line of research on the

ODE-inspired method. The basic idea is to use a high-order method for more accurate numerical solutions to the ODE. This leads to a larger ODE block that generates a sequence of intermediate approximations to the solution. We find that the larger ODE block is sufficient to take the role of several ODE blocks with first-order solutions. The benefit is obvious: the use of fewer ODE blocks lowers the risk of introducing errors in block switching, and the high-order method reduces the approximation error in each ODE block. See Figure 1 for a comparison of different models.

Our method is parameter-efficient because $\theta(t)$ is re-used within the same ODE block. As another "bonus", the model can be improved by learning coefficients of different intermediate approximations in a block. We evaluate our method in strong Transformer systems, covering both the wide (and big) model and the deep model. For machine translation tasks, ODE Transformer achieves 30.77 and 44.11 BLEU scores on the WMT'14 En-De and En-Fr test sets, setting a new state-of-the-art on the WMT'14 En-Fr task. It also significantly outperforms baselines on abstractive summarization and grammar error correction tasks.

2 Transformer and ODEs

We start with a description of Transformer, followed by its relationship with ODEs. We choose Transformer for our discussion and experiments because it is one of the state-of-the-art models in recent sentence generation tasks.

2.1 Transformer

Transformer is an example of the encoder-decoder paradigm (Vaswani et al., 2017). The encoder is a stack of identical layers. Each layer consists of a self-attention block and a feedforward network (FFN) block. Both of them equip with a residual connection and a layer normalization unit. Note that the term "block" is used in many different ways. In this paper, the term refers to any neural network that is enhanced by the residual connection (occasionally call it a *residual block*). Following the Pre-norm architecture (Wang et al., 2019), we define a block as

$$y_{t+1} = y_t + G(\mathrm{LN}(y_t), \theta_t) \quad (3)$$

where $\mathrm{LN}(\cdot)$ is the layer normalization function,[1] and $G(\cdot)$ is either the self-attention or feedforward network. The decoder shares a similar architecture, having an additional encoder-decoder attention block sandwiched between the self-attention and FFN blocks.

[1] We drop the parameter of $\mathrm{LN}(\cdot)$ for simplicity.

2.2 Ordinary Differential Equations

An ordinary differential equation is an equation involving a function $y(t)$ of a variable t and its derivatives. A simple form of ODE is an equation that defines the first-order derivative of $y(t)$, like

$$\frac{\mathrm{d}y(t)}{\mathrm{d}t} = f(y(t), t) \quad (4)$$

where $f(y(t), t)$ defines a time-dependent vector field if we know its value at all points of y and all instants of time t. Eq. (4) covers a broad range of problems, in that the change of a variable is determined by its current value and a time variable t. This formulation also works with Pre-norm Transformer blocks. For notational simplicity, we re-define $G(\mathrm{LN}(y_t), \theta_t)$ as a new function $F(y_t, \theta_t)$:

$$F(y_t, \theta_t) = G(\mathrm{LN}(y_t), \theta_t)) \quad (5)$$

We then relax y_t and θ_t to continuous functions $y(t)$ and $\theta(t)$, and rewrite Eq. (3) to be:

$$y(t + \Delta t) = y(t) + \Delta t \cdot F(y(t), \theta(t)) \quad (6)$$

where Δt is the change of t, and is general called *step size*. Obviously, we have $\Delta t = 1$ in Transformer. But we can adjust step size Δt using a limit, and have

$$\lim_{\Delta t \to 0} \frac{y(t + \Delta t) - y(t)}{\Delta t} = F(y(t), \theta(t)) \quad (7)$$

Given the fact that $\lim_{\Delta t \to 0} \frac{y(t+\Delta t)-y(t)}{\Delta t} = \frac{\mathrm{d}y(t)}{\mathrm{d}t}$, Eq. (7) is an instance of Eq. (4). The only difference lies in that we introduce $\theta(t)$ into the right-hand side of Eq. (4). Then, we say that a Pre-norm Transformer block describes an ODE. It has been found that Eq. (3) shares the same form as the Euler method of solving the ODE described in Eq. (7) (Haber and Ruthotto, 2017). This establishes a relationship between Transformer and ODEs, in that, given $F(\cdot, \cdot)$ and learned parameters $\{\theta_t\}$, the forward pass of a multi-block Transformer is a process of running the Euler method for several steps.

3 The ODE Transformer

In numerical methods of ODEs, we want to ensure the precise solutions to the ODEs in a minimum number of computation steps. But the Euler method is not "precise" because it is a first-order method, and naturally with local truncation errors. The global error might be larger if we run it for a number of times.[2] This is obviously the case for Transformer, especially when the multi-layer neural network arises a higher risk of unstability in solving the ODEs (Haber and Ruthotto, 2017).

3.1 High-Order ODE Solvers

Here we use the Runge-Kutta methods for a higher order solution to ODEs (Runge, 1895; Kutta, 1901; Butcher, 1996; Ascher and Petzold, 1998). They are a classic family of iterative methods with different orders of precision.[3] More formally, the explicit Runge-Kutta methods of an n-step solution is defined to be:

$$
\begin{aligned}
y_{t+1} &= y_t + \sum_{i=1}^{n} \gamma_i F_i && (8)\\
F_1 &= h f(y_t, t) && (9)\\
F_i &= h f(y_t + \sum_{j=1}^{i-1} \beta_{ij} F_j, t + \alpha_i h) && (10)
\end{aligned}
$$

where h is the step size and could be simply 1 in most cases. F_i is an intermediate approximation to the solution at step $t + \alpha_i h$. α, β and γ are coefficients which can be determined by the Taylor series of y_{t+1} (Butcher, 1963). Eq. (10) describes a sequence of solution approximations $\{F_1, ..., F_n\}$ over n steps $\{t + \alpha_1 h, ..., t + \alpha_n h\}$. These approximations are then interpolated to form the final solution, as in Eq. (8).

The Runge-Kutta methods are straightforwardly applicable to the design of a Transformer block. All we need is to replace the function f (see Eq. (10)) with the function F (see Eq. (5)). The advantage is that the function F is re-used in a block. Also, the model parameter θ_t can be shared within the block.[4] In this way, one can omit $t + \alpha_i h$ in Eq. (10), and compute F_i by

$$
F_i = F(y_t + \sum_{j=1}^{i-1} \beta_{ij} F_j, \theta_t) \qquad (11)
$$

[2]The global error is what we would ordinarily call the error: the difference between $y(t)$ and the true solution. The local error is the error introduced in a single step: the difference between $y(t)$ and the solution obtained by assuming that $y(t-1)$ is the true solution

[3]A p-order numerical method means that the global truncation error is proportional to p power of the step size.

[4]Although we could distinguish the parameters at different steps in a block, we found that it did not help and made the model difficult to learn.

This makes the system more parameter-efficient. As would be shown in our experiments, the high-order Runge-Kutta methods can learn strong NMT systems with significantly smaller models.

The Runge-Kutta methods are general. For example, the Euler method is a first-order instance of them. For a second-order Runge-Kutta (RK2) block, we have

$$
\begin{aligned}
y_{t+1} &= y_t + \frac{1}{2}(F_1 + F_2) && (12)\\
F_1 &= F(y_t, \theta_t) && (13)\\
F_2 &= F(y_t + F_1, \theta_t) && (14)
\end{aligned}
$$

This is also known as the improved Euler method. Likewise, we can define a fourth-order Runge-Kutta (RK4) block to be:

$$
\begin{aligned}
y_{t+1} &= y_t + \\
&\quad \frac{1}{6}(F_1 + 2F_2 + 2F_3 + F_4) && (15)\\
F_1 &= F(y_t, \theta_t) && (16)\\
F_2 &= F(y_t + \frac{1}{2}F_1, \theta_t) && (17)\\
F_3 &= F(y_t + \frac{1}{2}F_2, \theta_t) && (18)\\
F_4 &= F(y_t + F_3, \theta_t) && (19)
\end{aligned}
$$

See Figure 2 for a comparison of different Runge-Kutta blocks. It should be noted that the method presented here can be interpreted from the perspective of representation refinement (Greff et al., 2017). It provides a way for a function to update the function itself. For example, Universal Transformer refines the representation of the input sequence using the same function and the same parameters in a block-wise manner (Dehghani et al., 2019). Here we show that inner block refinements can be modeled with a good theoretical support.

3.2 Coefficient Learning

In our preliminary experiments, the RK2 and RK4 methods yielded promising BLEU improvements when the model was shallow. But it was found that the improvements did not persist for deeper models. To figure out why this happened, let us review the Runge-Kutta methods from the angle of training. Take the RK2 method as an example. We rewrite Eq. (12) by substituting F_1 and F_2, as follow

$$
\begin{aligned}
y_{t+1} &= y_t + \frac{1}{2}F(y_t, \theta_t) + \\
&\quad \frac{1}{2}F(y_t + F(y_t, \theta_t), \theta_t) && (20)
\end{aligned}
$$

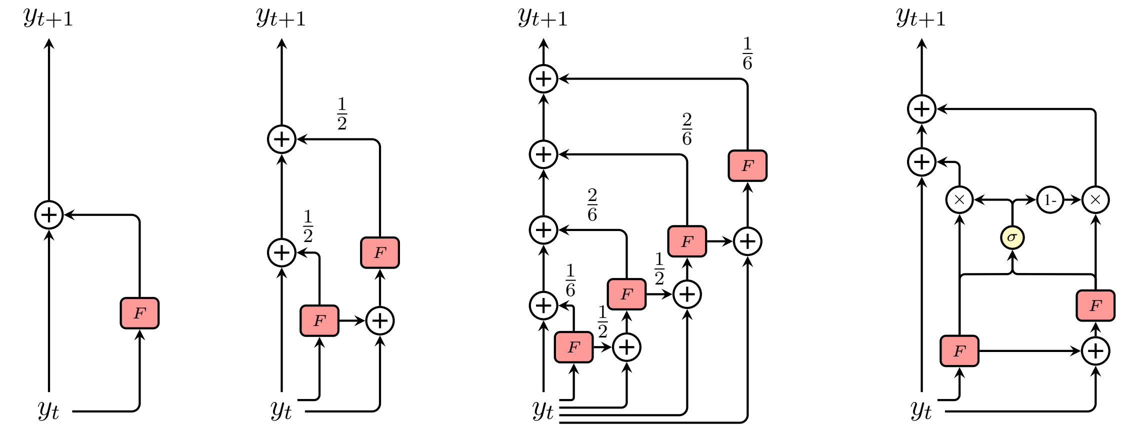

(a) Residual block (b) RK2-block (c) RK4-block (d) RK2-block (learnable γ_i)

Figure 2: Architectures of ODE Transformer blocks.

Let $\mathcal{E}$ be the loss of training, L be the number blocks of the model, and y_L be the model output. The gradient of $\mathcal{E}$ at y_t is

$$\frac{\partial \mathcal{E}}{\partial y_t} = \frac{\partial \mathcal{E}}{\partial y_L} \cdot \frac{1}{2^{L-t}} \cdot \prod_{k=t}^{L-1} (1 + g_k) \quad (21)$$

where

$$g_k = \left(1 + \frac{\partial F(y_k, \theta_k)}{\partial y_k}\right) \cdot \left(1 + \frac{\partial F(y_k + F(y_k, \theta_k), \theta_k)}{\partial y_k + F(y_k, \theta_k)}\right) \quad (22)$$

Seen from Eq. (21), $\frac{\partial \mathcal{E}}{\partial y_t}$ is proportional to the factor $\frac{1}{2^{L-t}}$. This leads to a higher risk of gradient vanishing when L is larger.

The problem somehow attributes to the small coefficients of F_i, that is, $\gamma_1 = \gamma_2 = \frac{1}{2}$. A natural idea is to empirically set $\gamma_i = 1$ to eliminate the product factor of less than 1 in gradient computation, although this is not theoretically grounded in standard Runge-Kutta methods. We rewrite Eq. (20) with the new coefficients, as follows

$$y_{t+1} = y_t + F(y_t, \theta_t) + F(y_t + F(y_t, \theta_t), \theta_t) \quad (23)$$

Then, we have the gradient, like this

$$\frac{\partial \mathcal{E}}{\partial y_t} = \frac{\partial \mathcal{E}}{\partial y_L} \cdot \prod_{k=t}^{L-1} g_k \quad (24)$$

This model is easy to optimize because $\frac{\partial \mathcal{E}}{\partial y_L}$ can be passed to lower-level blocks with no scales. Note that, the methods here are instances of parameter sharing (Dehghani et al., 2019; Lan et al., 2020). For example, in each ODE block, we use the same function F with the same parameter θ_t for all intermediate steps. Setting $\gamma_i = 1$ is a further step towards this because F_i is passed to next steps with the same scale. Here we call it implicit parameter sharing.

Another way of scaling F_i to further improve ODE functions is to learn the coefficients automatically on the training data. The simplest method is to initialize $\gamma_i = 1$ and independently optimize each scale. It helps the system learn the way of flowing F_i in a block. Based on it, scaling F_i by a weighted gate mechanism (Srivastava et al., 2015) empirically achieves the best performance (see Section 4). Take RK2-block as an instance, the concatenation of F_1 and F_2 is transformed to a scalar $(0, 1)$ through a sigmoid gate, then the block output y_{t+1} is

$$y_{t+1} = y_t + g \cdot F_1 + (1 - g) \cdot F_2 \quad (25)$$
$$g = \mathrm{sigmoid}([F_1, F_2] \cdot W + b) \quad (26)$$

where $[,]$ denotes the concatenation operation and W, b are learnable parameters. We call it RK2-block (learnable γ_i), and the architecture is shown in Figure 2 (d). This kind of formulation offers a more flexible way to decide which part contributes more and is also easy to be optimized. Moreover, we also summarize the comparison of various scaling functions in Appendix C.

3.3 Efficiency Discussion

ODE Transformer is efficient to use. As we only apply the ODE design schema into the encoder side, it only brings minor impacts on the inference

Model	Layers	WMT En-De				WMT En-Fr			
		#Param	Steps	BLEU	SBLEU	#Param	Steps	BLEU	SBLEU
Transformer (Vaswani et al., 2017)	6-6	213M	100K	28.40	-	222M	300K	41.00	-
MacaronNet (Lu et al., 2019)	6-6	-	-	30.20	-	-	-	-	-
Depth growing (Wu et al., 2019)	8-8	270M	800K	29.92	-	-	-	43.27	-
Transformer-DLCL (Wang et al., 2019)	30-6	137M	50K	29.30	28.6	-	-	-	-
Multiscale Collaborative (Wei et al., 2020)	18-6	512M	300K	30.56	-	-	-	-	-
ADMIN (Liu et al., 2020a)	60-12	262M	250K	30.01	29.5	-	250K	43.80	41.8
SDT (Li et al., 2020)	48-6	192M	50K	30.21	29.0	198M	100K	43.28	41.5
BERT-fused model (Zhu et al., 2020)	6-6	-	-	30.75	-	-	-	43.78	-
Base and Deep Models									
Residual-block	6-6	61M	50K	27.89	26.8	69M	100K	41.05	39.1
RK2-block	6-6	61M	50K	28.67	27.5	69M	100K	42.08	40.1
RK2-block (learnable γ_i)	6-6	61M	50K	28.89	27.7	69M	100K	42.31	40.3
RK4-block	6-6	61M	50K	29.03	27.9	69M	100K	42.56	40.6
Residual-block	24-6	118M	50K	29.43	28.3	123M	100K	42.67	40.6
RK2-block	24-6	118M	50K	29.85	28.7	123M	100K	43.04	41.1
RK2-block (learnable γ_i)	24-6	118M	50K	**30.29**	**29.2**	123M	100K	**43.48**	**41.5**
RK4-block	24-6	118M	50K	29.80	28.8	123M	100K	43.28	41.3
Wide Models									
Residual-block-Big	6-6	211M	100K	29.21	28.1	221M	100K	42.89	40.9
RK2-block	6-6	211M	100K	30.11	29.0	221M	100K	43.34	41.3
RK2-block (learnable γ_i)	6-6	211M	100K	30.53	29.4	221M	100K	43.59	41.6
RK4-block	6-6	211M	100K	30.39	29.3	221M	100K	43.55	41.6
Residual-block-Big	12-6	286M	100K	29.91	28.9	297M	100K	43.22	41.2
RK2-block	12-6	286M	100K	30.58	29.4	297M	100K	43.88	42.0
RK2-block (learnable γ_i)	12-6	286M	100K	**30.77**	**29.6**	297M	100K	**44.11**	**42.2**
RK4-block	12-6	286M	100K	30.55	29.4	297M	100K	43.81	41.9

Table 1: Comparison with the state-of-the-arts on the WMT En-De and WMT En-Fr tasks. We both report the tokenized BLEU and SacreBLEU scores for comparison with previous work.

Model	Params	Epochs	BLEU
Transformer in Mehta et al. (2020)	62M	170	34.30
DeLight (Mehta et al., 2020)	53M	170	34.70
Int Transformer† (Lin et al., 2020)	-	-	32.60
Transformer (Our impl.)	69M	20	33.49
RK2-block (learnable γ_i)	69M	20	34.94
RK2-block-Big (learnable γ_i)	226M	20	**35.28**

Table 2: Results on the WMT En-Ro task. † indicates the related information is not reported.

Model	Params	BLEU
Transformer (Vaswani et al., 2017)	62M	27.30
Evolved Transformer (So et al., 2019)	46M	27.70
Lite Transformer† (Wu et al., 2020)	-	26.50
DeLight (Mehta et al., 2020)	37M	27.60
RK2-block (learnable γ_i, H=256, L=28)	37M	**28.24**
RK2-block (learnable γ_i, H=256, L=18)	29M	27.84

Table 3: The comparison of model efficiency on the WMT En-De task.

speed due to the autoregressive decoding schema. Another concern here is the memory consumption. ODE Transformer consumes more memory than the baseline in the same depth since we need to store the intermediate approximations in the forward pass. But the additional consumption is less than that of the baseline who has the same computation cost. We give a quantitative analysis in Section 5.

4 Experimental Results

Due to the limited space, the details of experimental setups could be found in Appendix A and B.

Results of En-De and En-Fr Table 1 compares ODE Transformer with several state-of-the-art systems. Both RK2-block and RK4-block outperform the baselines by a large margin with different model capacities. For example, RK2-block obtains a +1.00 BLEU improvement with the base configuration when the depth is 6. RK4-block yields a gain of 0.17 BLEU points on top of RK2-block. This observation empirically validates the conjecture that high-order ODE functions are more efficient. When we switch to deep models, our method is more parameter efficient. E.g., RK2-block is comparable with a strong 48-layer system (Li et al., 2020) with half of the encoder depth. Similarly,

Model	Summarization			Correction		
	RG-1	RG-2	RG-L	Prec.	Recall	$F_{0.5}$
Liu et al. (2020b)	41.00	18.30	37.90	66.80	35.00	56.60
Residual-block	40.47	17.73	37.29	67.97	32.17	55.61
RK2-block	41.58	18.57	38.41	**68.21**	35.30	57.49
RK4-block	**41.83**	**18.84**	**38.68**	66.20	**38.13**	**57.71**

Table 4: Results of ODE Transformer on the summarization and correction tasks.

Model	1-Layer	2-Layer
Residual-Block	142.33	136.07
RK2-block	131.80	123.12
RK2-block ($\gamma_i = 1$)	132.67	123.90
RK2-block (learnable γ_i)	128.48	121.02
RK4-block	**126.89**	**119.46**

Table 5: Comparison of PPL on systems with different ODE blocks.

Model	Depth	Inference		Memory	
		Base	Big	Base	Big
Residual-Block	6	147.1	98.7	7.2	13.2
Residual-Block	12	141.3	94.5	10.9	18.7
Residual-Block	24	122.0	87.3	14.1	23.5
RK2-Block	6	141.6	93.9	8.5	15.1
RK4-Block	6	124.8	87.1	9.7	18.2

Table 6: Comparison of inference speed (sentences/s) and memory consumption (G).

wide models can also benefit from the enlarging layer depth (Wei et al., 2020; Li et al., 2020). RK2-block achieves BLEU scores of 30.77 and 44.11 on the En-De and the En-Fr tasks, significantly surpassing the standard Big model by 1.32 and 0.70 BLEU points. This sets a new state-of-the-art on these tasks with fewer parameters.

Results of En-Ro Table 2 exhibits model parameters, total training steps and BLEU scores of several strong systems on the En-Ro task. Again, ODE Transformer outperforms these baselines. As stated in (Mehta et al., 2020), they trained the model up to 170 epochs and obtained a BLEU score of 34.70 through the `DeLight` model. However, the observation here is quite different. The validation PPL begins to increase after 20 epochs. Thus, our baseline is slightly inferior to theirs, but matches the result reported in Lin et al. (2020). ODE blocks achieve even better performance with `DeLight` within much less training cost. For a bigger model (line 6), it obtains a BLEU score of 35.28.

Parameter Efficiency Table 3 summaries the results of several efficient Transformer variants, including Lite Transformer (Wu et al., 2020), DeLight (Mehta et al., 2020) and a light version of the Evolved Transformer (So et al., 2019). As expected, ODE Transformer is promising for smaller models. It is comparable in BLEU with `DeLight` but having 9M fewer parameters. Under the same model capacity, it outperforms `DeLight` by 0.64 BLEU points. It may offer a new choice for deploying NMT systems on edge devices.

Results of Summarization and Correction We also evaluated the ODE Transformer on another two sequence generation tasks. Table 4 shows that both RK2-block and RK4-block outperform the baselines by a margin. Similarly, RK4-block is more superior to RK2-block when the model is shallow. More results and case studies could be found in Appendix C.

5 Analysis

Here we investigate some interesting issues. For simplicity to lengend, we call RK2-block with coefficients initialized by 1 as RK2-block-v1, and learnable coefficients (Eq. (25)) as RK2-block-v2.

Quantization of the Truncation Error Actually, we cannot obtain the "true" solution of each block output in NMT, because we mainly experimented on the encoder side. Instead, we tested our system on the language modeling task, where the perplexity between the single layer model output and the ground truth could be regarded as the truncation error with no error propagations. Table 5 shows the perplexities on the Penn Treebank dataset (Mikolov et al., 2011). All ODE Transformer variants reduce the errors significantly. RK4-order achieves the lowest PPL on both settings. In addition, RK2-block can even obtain a lower PPL than a 2-layer residual-block. The observation here again verifies larger ODE blocks behave superior to the standard residual-block.

Inference Speed and Memory Consumption Table 6 shows the comparison of inference speed and memory consumption discussed in Section 3.3. Experimental results demonstrate the proposed ODE design schema results in acceptable inference speeds. And it is also memory friendly through the memory comparison between the baseline and the RK variants in both base and big configurations.

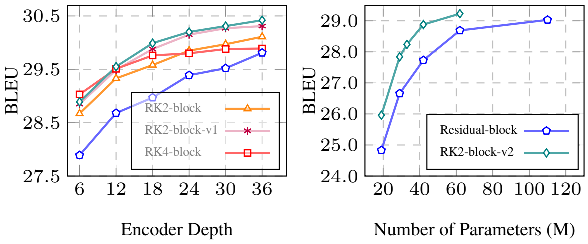

Figure 3: The comparison of BLEU against different encoder depth and the number of model parameters.

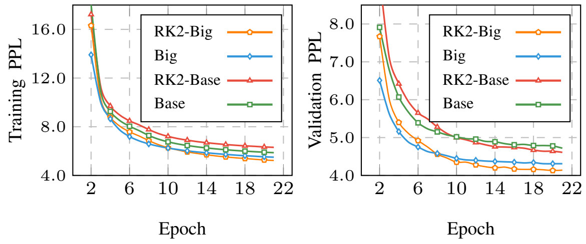

Figure 5: The comparison of training and validation PPL on base and wide models.

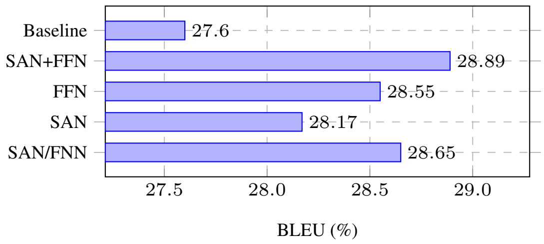

Figure 4: BLEU scores [%] of several $F(\cdot,\cdot)$ on the WMT En-De task.

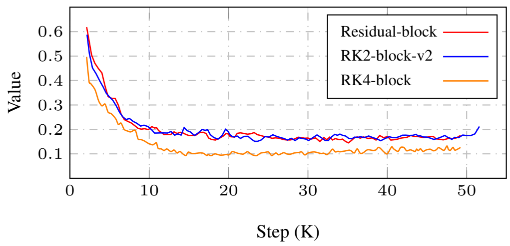

Figure 6: Visualization of the gradient norm of ODE Transformers compared with the baseline.

BLEU against Encoder Depth Figure 3 (left) depicts BLEU scores of several ODE Transformer variants and the baseline under different encoder depths. All ODE Transformer variants are significantly superior to the baseline when depth ≤ 24 . RK2-block-v2 almost achieves the best performance over all depths, especially when the model becomes deeper. Interestingly, Figure 3 confirms again that ODE Transformer is parameter efficient, e.g., a 6-layer RK2-block is comparable with the 18-layer baseline system. Another finding here is RK4-block performs well on shallow models, but it is inferior to RK2-block when the depth is going deep. This is because original coefficients may cause the optimization problem in the backward propagation in deep models (see Section 3.2). Also, Figure 3 (right) plots BLEU as a function of the model size when the hidden size is 256. The RK2 method significantly surpasses the baseline using much fewer parameters.

Ablation Study on Different $F(\cdot,\cdot)$ As stated in Section 3, the $F(\cdot,\cdot)$ function can either be SAN, FFN or both of them (SAN+FFN). As shown in Figure 4, high-order ODE works better with FFN than SAN. An explanation might be that the FFN component has more parameters than the SAN component.[5] The model that treats FFN and SAN as a single ODE block behaves the best.

[5]There are $2 \cdot d_{\text{model}} \cdot 4d_{\text{model}}$ parameters in FFN and $d_{\text{model}} \cdot 3d_{\text{model}} + d_{\text{model}} \cdot d_{\text{model}}$ in SAN.

Training and Validation Perplexity Figure 5 plots the training and validation PPL curves of RK blocks and the baseline enhanced by RPR (Shaw et al., 2018). RK2-block obtains lower training and validation PPLs in both configurations (base and wide models).

Visualization of the Gradient Norm We also collect the gradient information of several well-trained systems during training. Figure 6 plots the gradient norm of RK2-block-v2, RK4-block and the standard residual-block (baseline). As we can see that Pre-Norm residual block is able to make the training stable (Wang et al., 2019). Both RK2-block-v2 and RK4-block provide richer signals due to the implicit parameter sharing among intermediate approximations. The two learning curves appear to be nearly the same, which is consistent with the results in Table 1.

Comparison of Different ODE Design Schemas Then, we take a comprehensive analysis of several ODE design schemas. As stated in Lu et al. (2018)'s work, several models in computer vision, such as LeapfrogNet (He et al., 2019), PolyNet (Zhang et al., 2017) and MultistepNet (Lu et al., 2018), can also be interpreted from the ODE perspective. The related ODE functions are summarized in Table 7. We re-implemented these methods using the same codebase for fair comparisons. We conducted experiments following the base configuration on the En-De task.

Model	Information Flow	Related ODEs	BLEU
Leapfrog (He et al., 2019)	$y_{t+1} = y_{t-1} + 2F(y_t, \theta_t)$	Multistep Euler	28.07
Multistep (Lu et al., 2018)	$y_{t+1} = k_n \cdot y_t + (1 - k_n) \cdot y_{t-1} + F(y_t, \theta_t)$	Multistep Euler	28.17
DLCL (Wang et al., 2019)	$y_{t+1} = y_0 + \sum_{l=0}^{t} W_l F(y_l, \theta_l)$	Multistep Euler	27.78
PolyNet (Zhang et al., 2017)	$y_{t+1} = y_t + F(y_t, \theta_t) + F(F(y_t, \theta_t), \theta_t)$	Backward Euler	28.15
RK2-block	$y_{t+1} = y_t + \frac{1}{2}F(y_t, \theta_t) + \frac{1}{2}F(y_t + F(y_t, \theta_t), \theta_t)$	Improved Euler	28.67
RK2-block ($\gamma_i = 1$)	$y_{t+1} = y_t + F(y_t, \theta_t) + F(y_t + F(y_t, \theta_t), \theta_t)$	RK 2nd-order	28.77
RK2-block (learnable γ_i)	$y_{t+1} = y_t + \gamma_1 \cdot F(y_t, \theta_t) + \gamma_2 \cdot F(y_t + F(y_t, \theta_t), \theta_t)$	RK 2nd-order	28.86
RK4-block	$y_{t+1} = y_t + \frac{1}{6}F_1 + \frac{2}{6}F_2 + \frac{2}{6}F_3 + \frac{1}{6}F_4$	RK 4th-order	29.03

Table 7: Comparison of several ODE-inspired design schemas on the En-De task. We re-implement and apply these methods into Transformer. Note that y_n denotes the model input of layer n. Due to the limited space, we use F_i to denote the intermediate representation, where $i \in [1, 4]$.

At time t, Multistep Euler methods requires previous states, e.g. y_{t-1}, to generate the current approximation, instead of iterative refinements based on the current-time state. So these methods are heavier than ODE Transformer. Note that DLCL (Wang et al., 2019) can also be regarded as a multistep Euler method, which is more competitive in deep Transformer. But there is just a modest improvement upon the shallow baseline. Theoretically, the Backward Euler method is slightly better than the Forward Euler method in numerical analysis, but the improvement is marginal. Note that our ODE Transformer achieves consistent BLEU improvements over the aforementioned methods. The reason is that such iterative refinements provide more efficient and effective parameters learning.

6 Related Work

Deep Transformer models Recently, deep Transformer has witnessed tremendous success in machine translation. A straightforward way is to shorten the path from upper-level layers to lower-level layers thus to alleviate the gradient vanishing or exploding problems (Bapna et al., 2018; Wang et al., 2019; Wu et al., 2019; Wei et al., 2020). For deeper models, the training cost is nonnegligible. To speed up the training, an alternative way is to train a shallow model first and progressively increasing the model depth (Li et al., 2020; Dong et al., 2020). Apart from the model architecture improvements, another way of easing the optimization is to utilize carefully designed parameter initialization strategies (Zhang et al., 2019; Xu et al., 2020; Huang et al., 2020; Liu et al., 2020a). Note that ODE Transformer is orthogonal to the aforementioned methods, and we will test it on these methods in the future work.

Ordinary Differential Equations The relationship between ResNet and ODEs was first proposed by Weinan (2017). This shows a brand-new perspective on the design of effective deep architectures. Moreover, the success of Neural ODENet (Chen et al., 2018) have attracted researchers. Some insightful architectures (Zhang et al., 2017; Larsson et al., 2017; Lu et al., 2018; He et al., 2019; Zhu and Fu, 2018; Lu et al., 2019; Sander et al., 2021) can also be interpreted from the ODE perspective. But, in NLP, it is still rare to see studies on designing models from the ODE perspective. Zhang et al. (2021) proposed continuous self-attention models using the same merit with neural ODE. Perhaps the most relevant work with us is an (2021)'s work. They redesigned the Transformer architecture from a multi-particle dynamic system view in terms of efficiency. Unlike them, we show that the stacked first-order ODE blocks may cause error accumulation, thus hindering the model performance. We address this issue by introducing high-order blocks, and demonstrate significant performance improvements on three sequence generation tasks, which is complementary to Baier-Reinio and De Sterck (2020)'s work.

7 Conclusions

This paper explores the relationship between Transformer and ODEs. We propose ODE Transformer to help the model benefit from high-order ODE solutions. Experimental results on the three representative sentence generations tasks (i.e., machine translation, abstractive summarization, and grammatical error correction) show the effectiveness and efficiency of ODE Transformer. It achieves 30.77 and 44.11 BLEU scores on the WMT'14 En-De and En-Fr benchmarks, setting a new state-of-the-art result on the En-Fr.

References

Subhabrata Dutta an. 2021. Redesigning the transformer architecture with insights from multi-particl. *ArXiv preprint*, abs/2109.15142.

Uri M Ascher and Linda R Petzold. 1998. *Computer methods for ordinary differential equations and differential-algebraic equations*, volume 61. Siam.

Aaron Baier-Reinio and Hans De Sterck. 2020. N-ode transformer: A depth-adaptive variant of the transformer using neural ordinary differential equations. *ArXiv preprint*, abs/2010.11358.

Ankur Bapna, Mia Chen, Orhan Firat, Yuan Cao, and Yonghui Wu. 2018. Training deeper neural machine translation models with transparent attention. In *Proceedings of the 2018 Conference on Empirical Methods in Natural Language Processing*, pages 3028–3033, Brussels, Belgium. Association for Computational Linguistics.

Christopher Bryant, Mariano Felice, and Ted Briscoe. 2017. Automatic annotation and evaluation of error types for grammatical error correction. In *Proceedings of the 55th Annual Meeting of the Association for Computational Linguistics (Volume 1: Long Papers)*, pages 793–805, Vancouver, Canada.

John C Butcher. 1963. Coefficients for the study of runge-kutta integration processes. *Journal of the Australian Mathematical Society*, 3(2):185–201.

John Charles Butcher. 1996. A history of runge-kutta methods. *Applied numerical mathematics*, 20(3):247–260.

Bo Chang, Lili Meng, Eldad Haber, Lars Ruthotto, David Begert, and Elliot Holtham. 2018. Reversible architectures for arbitrarily deep residual neural networks. In *Proceedings of the Thirty-Second AAAI Conference on Artificial Intelligence, (AAAI-18), the 30th innovative Applications of Artificial Intelligence (IAAI-18), and the 8th AAAI Symposium on Educational Advances in Artificial Intelligence (EAAI-18), New Orleans, Louisiana, USA, February 2-7, 2018*, pages 2811–2818. AAAI Press.

Tian Qi Chen, Yulia Rubanova, Jesse Bettencourt, and David Duvenaud. 2018. Neural ordinary differential equations. In *Advances in Neural Information Processing Systems 31: Annual Conference on Neural Information Processing Systems 2018, NeurIPS 2018, December 3-8, 2018, Montréal, Canada*, pages 6572–6583.

Shamil Chollampatt and Hwee Tou Ng. 2018. A multilayer convolutional encoder-decoder neural network for grammatical error correction. In *Proceedings of the Thirty-Second AAAI Conference on Artificial Intelligence, (AAAI-18), the 30th innovative Applications of Artificial Intelligence (IAAI-18), and the 8th AAAI Symposium on Educational Advances in Artificial Intelligence (EAAI-18), New Orleans, Louisiana, USA, February 2-7, 2018*, pages 5755–5762. AAAI Press.

Zihang Dai, Zhilin Yang, Yiming Yang, Jaime Carbonell, Quoc Le, and Ruslan Salakhutdinov. 2019. Transformer-XL: Attentive language models beyond a fixed-length context. In *Proceedings of the 57th Annual Meeting of the Association for Computational Linguistics*, pages 2978–2988, Florence, Italy. Association for Computational Linguistics.

Mostafa Dehghani, Stephan Gouws, Oriol Vinyals, Jakob Uszkoreit, and Lukasz Kaiser. 2019. Universal transformers. In *7th International Conference on Learning Representations, ICLR 2019, New Orleans, LA, USA, May 6-9, 2019*. OpenReview.net.

Chengyu Dong, Liyuan Liu, Zichao Li, and Jingbo Shang. 2020. Towards adaptive residual network training: A neural-ode perspective. In *Proceedings of the 37th International Conference on Machine Learning, ICML 2020, 13-18 July 2020, Virtual Event*, volume 119 of *Proceedings of Machine Learning Research*, pages 2616–2626. PMLR.

Sebastian Gehrmann, Yuntian Deng, and Alexander Rush. 2018. Bottom-up abstractive summarization. In *Proceedings of the 2018 Conference on Empirical Methods in Natural Language Processing*, pages 4098–4109, Brussels, Belgium.

Klaus Greff, Rupesh Kumar Srivastava, and Jürgen Schmidhuber. 2017. Highway and residual networks learn unrolled iterative estimation. In *5th International Conference on Learning Representations, ICLR 2017, Toulon, France, April 24-26, 2017, Conference Track Proceedings*. OpenReview.net.

Eldad Haber and Lars Ruthotto. 2017. Stable architectures for deep neural networks. *Inverse Problems*, 34(1):014004.

Eldad Haber, Lars Ruthotto, Elliot Holtham, and Seong-Hwan Jun. 2018. Learning across scales - multiscale methods for convolution neural networks. In *Proceedings of the Thirty-Second AAAI Conference on Artificial Intelligence, (AAAI-18), the 30th innovative Applications of Artificial Intelligence (IAAI-18), and the 8th AAAI Symposium on Educational Advances in Artificial Intelligence (EAAI-18), New Orleans, Louisiana, USA, February 2-7, 2018*, pages 3142–3148. AAAI Press.

Kaiming He, Xiangyu Zhang, Shaoqing Ren, and Jian Sun. 2016. Deep residual learning for image recognition. In *2016 IEEE Conference on Computer Vision and Pattern Recognition, CVPR 2016, Las Vegas, NV, USA, June 27-30, 2016*, pages 770–778. IEEE Computer Society.

Xiangyu He, Zitao Mo, Peisong Wang, Yang Liu, Mingyuan Yang, and Jian Cheng. 2019. Ode-inspired network design for single image super-resolution. In *IEEE Conference on Computer Vision and Pattern Recognition, CVPR 2019, Long Beach, CA, USA, June 16-20, 2019*, pages 1732–1741. Computer Vision Foundation / IEEE.

Karl Moritz Hermann, Tomás Kociský, Edward Grefenstette, Lasse Espeholt, Will Kay, Mustafa Suleyman, and Phil Blunsom. 2015. Teaching machines to read and comprehend. In *Advances in Neural Information Processing Systems 28: Annual Conference on Neural Information Processing Systems 2015, December 7-12, 2015, Montreal, Quebec, Canada*, pages 1693–1701.

Xiao Shi Huang, Felipe Pérez, Jimmy Ba, and Maksims Volkovs. 2020. Improving transformer optimization through better initialization. In *Proceedings of the 37th International Conference on Machine Learning, ICML 2020, 13-18 July 2020, Virtual Event*, volume 119 of *Proceedings of Machine Learning Research*, pages 4475–4483. PMLR.

Diederik P. Kingma and Jimmy Ba. 2015. Adam: A method for stochastic optimization. In *3rd International Conference on Learning Representations, ICLR 2015, San Diego, CA, USA, May 7-9, 2015, Conference Track Proceedings*.

Wilhelm Kutta. 1901. Beitrag zur naherungsweisen integration totaler differentialgleichungen. *Z. Math. Phys.*, 46:435–453.

Zhenzhong Lan, Mingda Chen, Sebastian Goodman, Kevin Gimpel, Piyush Sharma, and Radu Soricut. 2020. ALBERT: A lite BERT for self-supervised learning of language representations. In *8th International Conference on Learning Representations, ICLR 2020, Addis Ababa, Ethiopia, April 26-30, 2020*. OpenReview.net.

Gustav Larsson, Michael Maire, and Gregory Shakhnarovich. 2017. Fractalnet: Ultra-deep neural networks without residuals. In *5th International Conference on Learning Representations, ICLR 2017, Toulon, France, April 24-26, 2017, Conference Track Proceedings*. OpenReview.net.

Bei Li, Ziyang Wang, Hui Liu, Yufan Jiang, Quan Du, Tong Xiao, Huizhen Wang, and Jingbo Zhu. 2020. Shallow-to-deep training for neural machine translation. In *Proceedings of the 2020 Conference on Empirical Methods in Natural Language Processing (EMNLP)*, pages 995–1005, Online. Association for Computational Linguistics.

Chin-Yew Lin. 2004. ROUGE: A package for automatic evaluation of summaries. In *Text Summarization Branches Out*, pages 74–81, Barcelona, Spain. Association for Computational Linguistics.

Ye Lin, Yanyang Li, Tengbo Liu, Tong Xiao, Tongran Liu, and Jingbo Zhu. 2020. Towards fully 8-bit integer inference for the transformer model. In *Proceedings of the Twenty-Ninth International Joint Conference on Artificial Intelligence, IJCAI 2020*, pages 3759–3765. ijcai.org.

Liyuan Liu, Xiaodong Liu, Jianfeng Gao, Weizhu Chen, and Jiawei Han. 2020a. Understanding the difficulty of training transformers. In *Proceedings of the 2020 Conference on Empirical Methods in Natural Language Processing (EMNLP)*, pages 5747–5763, Online. Association for Computational Linguistics.

Xuebo Liu, Longyue Wang, Derek F Wong, Liang Ding, Lidia S Chao, and Zhaopeng Tu. 2020b. Understanding and improving encoder layer fusion in sequence-to-sequence learning. *ArXiv preprint*, abs/2012.14768.

Yiping Lu, Zhuohan Li, Di He, Zhiqing Sun, Bin Dong, Tao Qin, Liwei Wang, and Tie-Yan Liu. 2019. Understanding and improving transformer from a multi-particle dynamic system point of view. *ArXiv preprint*, abs/1906.02762.

Yiping Lu, Aoxiao Zhong, Quanzheng Li, and Bin Dong. 2018. Beyond finite layer neural networks: Bridging deep architectures and numerical differential equations. In *Proceedings of the 35th International Conference on Machine Learning, ICML 2018, Stockholmsmässan, Stockholm, Sweden, July 10-15, 2018*, volume 80 of *Proceedings of Machine Learning Research*, pages 3282–3291. PMLR.

Sachin Mehta, Marjan Ghazvininejad, Srinivasan Iyer, Luke Zettlemoyer, and Hannaneh Hajishirzi. 2020. Delight: Very deep and light-weight transformer. *ArXiv preprint*, abs/2008.00623.

Tomáš Mikolov, Anoop Deoras, Stefan Kombrink, Lukáš Burget, and Jan Černockỳ. 2011. Empirical evaluation and combination of advanced language modeling techniques. In *Twelfth annual conference of the international speech communication association*.

Ramesh Nallapati, Bowen Zhou, Cícero Nogueira dos Santos, Çaglar Gülçehre, and Bing Xiang. 2016. Abstractive text summarization using sequence-to-sequence rnns and beyond. In *Proceedings of the 20th SIGNLL Conference on Computational Natural Language Learning, CoNLL 2016, Berlin, Germany, August 11-12, 2016*, pages 280–290. ACL.

Myle Ott, Sergey Edunov, Alexei Baevski, Angela Fan, Sam Gross, Nathan Ng, David Grangier, and Michael Auli. 2019. fairseq: A fast, extensible toolkit for sequence modeling. In *Proceedings of the 2019 Conference of the North American Chapter of the Association for Computational Linguistics (Demonstrations)*, pages 48–53, Minneapolis, Minnesota. Association for Computational Linguistics.

Carl Runge. 1895. Über die numerische auflösung von differentialgleichungen. *Mathematische Annalen*, 46(2):167–178.

Lars Ruthotto and Eldad Haber. 2019. Deep neural networks motivated by partial differential equations. *Journal of Mathematical Imaging and Vision volume*, 62:352–364.

Michael E. Sander, Pierre Ablin, Mathieu Blondel, and Gabriel Peyré. 2021. Momentum residual neural networks. In *Proceedings of the 38th International Conference on Machine Learning, ICML 2021, 18-24 July 2021, Virtual Event*, volume 139 of *Proceedings of Machine Learning Research*, pages 9276–9287. PMLR.

Abigail See, Peter J. Liu, and Christopher D. Manning. 2017. Get to the point: Summarization with pointer-generator networks. In *Proceedings of the 55th Annual Meeting of the Association for Computational Linguistics (Volume 1: Long Papers)*, pages 1073–1083, Vancouver, Canada.

Rico Sennrich, Barry Haddow, and Alexandra Birch. 2016. Neural machine translation of rare words with subword units. In *Proceedings of the 54th Annual Meeting of the Association for Computational Linguistics (Volume 1: Long Papers)*, pages 1715–1725, Berlin, Germany. Association for Computational Linguistics.

Peter Shaw, Jakob Uszkoreit, and Ashish Vaswani. 2018. Self-attention with relative position representations. In *Proceedings of the 2018 Conference of the North American Chapter of the Association for Computational Linguistics: Human Language Technologies, Volume 2 (Short Papers)*, pages 464–468, New Orleans, Louisiana. Association for Computational Linguistics.

David R. So, Quoc V. Le, and Chen Liang. 2019. The evolved transformer. In *Proceedings of the 36th International Conference on Machine Learning, ICML 2019, 9-15 June 2019, Long Beach, California, USA*, volume 97 of *Proceedings of Machine Learning Research*, pages 5877–5886. PMLR.

Rupesh Kumar Srivastava, Klaus Greff, and Jürgen Schmidhuber. 2015. Highway networks. *ArXiv preprint*, abs/1505.00387.

Ashish Vaswani, Noam Shazeer, Niki Parmar, Jakob Uszkoreit, Llion Jones, Aidan N. Gomez, Lukasz Kaiser, and Illia Polosukhin. 2017. Attention is all you need. In *Advances in Neural Information Processing Systems 30: Annual Conference on Neural Information Processing Systems 2017, December 4-9, 2017, Long Beach, CA, USA*, pages 5998–6008.

Qiang Wang, Bei Li, Tong Xiao, Jingbo Zhu, Changliang Li, Derek F. Wong, and Lidia S. Chao. 2019. Learning deep transformer models for machine translation. In *Proceedings of the 57th Annual Meeting of the Association for Computational Linguistics*, pages 1810–1822, Florence, Italy. Association for Computational Linguistics.

Xiangpeng Wei, Heng Yu, Yue Hu, Yue Zhang, Rongxiang Weng, and Weihua Luo. 2020. Multiscale collaborative deep models for neural machine translation. In *Proceedings of the 58th Annual Meeting of the Association for Computational Linguistics*, pages 414–426, Online. Association for Computational Linguistics.

E Weinan. 2017. A proposal on machine learning via dynamical systems. *Communications in Mathematics and Statistics*, 5(1):1–11.

Lijun Wu, Yiren Wang, Yingce Xia, Fei Tian, Fei Gao, Tao Qin, Jianhuang Lai, and Tie-Yan Liu. 2019. Depth growing for neural machine translation. In *Proceedings of the 57th Annual Meeting of the Association for Computational Linguistics*, pages 5558–5563, Florence, Italy. Association for Computational Linguistics.

Zhanghao Wu, Zhijian Liu, Ji Lin, Yujun Lin, and Song Han. 2020. Lite transformer with long-short range attention. In *8th International Conference on Learning Representations, ICLR 2020, Addis Ababa, Ethiopia, April 26-30, 2020*. OpenReview.net.

Hongfei Xu, Qiuhui Liu, Josef van Genabith, Deyi Xiong, and Jingyi Zhang. 2020. Lipschitz constrained parameter initialization for deep transformers. In *Proceedings of the 58th Annual Meeting of the Association for Computational Linguistics*, pages 397–402, Online. Association for Computational Linguistics.

Biao Zhang, Ivan Titov, and Rico Sennrich. 2019. Improving deep transformer with depth-scaled initialization and merged attention. In *Proceedings of the 2019 Conference on Empirical Methods in Natural Language Processing and the 9th International Joint Conference on Natural Language Processing (EMNLP-IJCNLP)*, pages 898–909, Hong Kong, China. Association for Computational Linguistics.

Jing Zhang, Peng Zhang, Baiwen Kong, Junqiu Wei, and Xin Jiang. 2021. Continuous self-attention models with neural ODE networks. In *Thirty-Fifth AAAI Conference on Artificial Intelligence, AAAI 2021, Thirty-Third Conference on Innovative Applications of Artificial Intelligence, IAAI 2021, The Eleventh Symposium on Educational Advances in Artificial Intelligence, EAAI 2021, Virtual Event, February 2-9, 2021*, pages 14393–14401. AAAI Press.

Xingcheng Zhang, Zhizhong Li, Chen Change Loy, and Dahua Lin. 2017. Polynet: A pursuit of structural diversity in very deep networks. In *2017 IEEE Conference on Computer Vision and Pattern Recognition, CVPR 2017, Honolulu, HI, USA, July 21-26, 2017*, pages 3900–3908. IEEE Computer Society.

Qingyu Zhou, Nan Yang, Furu Wei, Shaohan Huang, Ming Zhou, and Tiejun Zhao. 2018. Neural document summarization by jointly learning to score and select sentences. In *Proceedings of the 56th Annual Meeting of the Association for Computational Linguistics (Volume 1: Long Papers)*, pages 654–663, Melbourne, Australia.

Jinhua Zhu, Yingce Xia, Lijun Wu, Di He, Tao Qin, Wengang Zhou, Houqiang Li, and Tie-Yan Liu. 2020. Incorporating BERT into neural machine translation. In *8th International Conference on*

Learning Representations, ICLR 2020, Addis Ababa, Ethiopia, April 26-30, 2020. OpenReview.net.

Mai Zhu and Chong Fu. 2018. Convolutional neural networks combined with runge-kutta methods. *CoRR*, abs/1802.08831.

A Experimental Setups

Machine Translation We report results on three WMT benchmarks. For the WMT'14 English-German (En-De) task, the training data consisted of approximately 4.5M tokenized sentence pairs, as in (Vaswani et al., 2017). All sentences were segmented into sequences of sub-word units (Sennrich et al., 2016) with 32K merge operations using a shared vocabulary. We selected *newstest2013* as the validation data and *newstest2014* as the test data. For the WMT'14 English-French (En-Fr) task, we used the dataset provided within Fairseq, i.e., 36M training sentence pairs from WMT'14. *newstest2012+newstest2013* was the validation data and *newstest2014* was the test data. For the WMT'16 English-Romanian (En-Ro) task, we replicated the setup of (Mehta et al., 2020), which used 600K/2K/2K sentence pairs for training, evaluation and inference, respectively.

Abstractive Summarization We also tested the models's ability to process long sequences on the CNN-DailyMail summarization task (Nallapati et al., 2016; Hermann et al., 2015). The preprocessed method was the same as in (Ott et al., 2019). We used a shared BPE with 30K operations, resulting in a vocabulary of $32,580$ entries. The evaluation metric was F1-Rouge (Lin, 2004) (Rouge-1, Rouge-2 and Rouge-L).

Grammar Error Correction We borrowed the setup from Chollampatt and Ng (2018) and used the provided preprocessed script. Word-level dropout technique was also applied to prevent the overfitting problem.

Language Modeling Here, we introduce the details about the Penn Treebank dataset (Mikolov et al., 2011) and the corresponding configuration. It contains 88K, $3,370$ and $3,761$ sentences for training, validation and test. The vocabulary size was $10K$. To evaluate the truncation error, we set the layer depth of the language model to 1 or 2 for a comprehensive comparison. Assume the layer depth is 1, then the loss between the block output and the ground-truth can be regarded as the truncation error. It alleviates the influence of the error accumulation across different layers.

Table 8 summarizes the details of our datasets. We both present the sentences and tokens of each task. For the En-De and En-Fr tasks, the datasets used in this work could be found in `Fairseq`.[6] For the En-Ro task, we used the preprocessed dataset provided by `DeLight`.[7] Note that we only shared the target embedding and the softmax embedding instead of a shared vocabulary between the source side and the target side. The CNN/DailyMail dataset consists of CNN stories[8] and Daily emails[9]. For the grammar error correction task (GEC), we conducted experiments on the CONLL dataset [10].

B Training and Evaluation

Training As suggested in Li et al. (2020)'s work, we adopted relative positional representation (RPR) (Shaw et al., 2018) for stronger baselines. All experiments were trained on 8 GPUs, with $4,096$ tokens on each GPU. For the En-De and the En-Fr tasks, we employed the gradient accumulation strategy with a step of 2 and 8, respectively. We used the Adam optimizer (Kingma and Ba, 2015) whose hyperparameters were set to $(0.9, 0.997)$. The hyperparameters including the learning rate, the warmup step and the total training steps of three tasks could be found in Table 8. It is noteworthy that we trained Base/Deep and Big models for 50K and 100K steps on the En-De task. We regarded merging SAN and FFN as the default ODE block. In addition, main results were the average of three times running with different random seeds, and we averaged the last 5/10 checkpoints for fair comparisons with previous work.

Since the proposed method is orthogonal to the model capacity, we evaluated the ODE Transformer on Base/Deep/Wide configurations, respectively. The detail of each configuration is as follows:

- Base/Deep Model. The hidden size of self-

[6] https://github.com/pytorch/fairseq/tree/master/examples/scaling_nmt

[7] https://github.com/sacmehta/delight/blob/master/readme_files/nmt/wmt16_en2ro.md

[8] https://drive.google.com/uc?export=download&id=0BwmD_VLjROrfTHk4NFg2SndKcjQ

[9] https://drive.google.com/uc?export=download&id=0BwmD_VLjROrfM1BxdkxVaTY2bWs

[10] https://www.cl.cam.ac.uk/research/nl/bea2019st

Model	Vocab	Dataset			Training					Inference	
		Train	Dev	Test	Lr	Warmup	Batch	Steps	WD	Beam	LP
WMT'14 En-De	34040	4.5M	3000	3003	0.002	16000	80K	50K	×	4	0.6
WMT'14 En-Fr	44424	35.7M	26822	3003	0.002	16000	320K	100K	×	4	0.6
WMT'16 En-Ro	34976	602K	1999	1999	0.002	8000	80K	17K	×	5	1.3
CNN/DailyMail	32584	287K	13368	11490	0.002	8000	160K	50K	×	4	2.0
CONLL	33136	827K	5448	1312	0.0015	4000	160K	15K	✓	6	0.6

Table 8: Statistics of the datasets and hyperparameters for three sequence generation tasks. For the dataset, we both report the vocabulary size, sentence numbers of training, validation and test sets. For the training, Lr denotes the peaking learning rate and Warmup denotes the warmup step of the Adam optimizer. WD denotes whether we applied word dropout. For the inference, Beam and LP denote the beam size and length penalty, respectively.

attention was 512, and the dimension of the inner-layer in FFN was $2,048$. We used 8 heads for attention. For training, we set all dropout to 0.1 as default, including residual dropout, attention dropout, ReLU dropout. Label smoothing $\epsilon_{ls} = 0.1$ was applied to enhance the generation ability of the model. For deep models, we only enlarged the encoder depth considering the inference speed.

- Wide (or Big) Model. We used the same architecture as Transformer-Base but with a larger hidden layer size $1,024$, more attention heads (16), and a larger feed forward inner-layer ($4,096$ dimensions). The residual dropout was set to 0.3 for the En-De task and 0.1 for the En-Fr task.

For the language modeling task, the hidden size was 512, and the filter size of the FFN was $2,048$. We set all the dropout rate as 0.1, including the residual dropout, attention dropout and the ReLU dropout. Each model was trained up to 20 epochs, and most models achieved the lowest PPL on the validation set when the epoch is 10. Then the validation PPL began to increase, though the training PPL is still declining. The warmup step was $2,000$ and the batch size was $4,096$. The max learning rate was set to 0.0007.

Evaluation For machine translation, we measured performance in terms of BLEU. Both tokenized BLEU and SacreBLEU[11] scores were reported on the En-De and En-Fr tasks. Also, we reported tokenized BLEU scores on the En-Ro task. In addition, we measured Rouge-1, Rouge-2, Rouge-L for CNN/DailyMail and precision, recall, $F_{0.5}$ for CONLL. The beam size and length penalty of each task are summarized in Table 8.

C Additional Results and Analyses

Comparison on the CNN/DailyMail Dataset We summarize the previous results on the CNN/DailyMail dataset (See Table 9). The performance was evaluated by ROUGE-1, ROUGE-2 and ROUGE-L, respectively. Intuitively, high-order ODE functions can significantly improve on top of the Euler method as well as several strong existing models.[12] Again, RK4-block beats the baseline and RK2-block by up to 1.36 and 0.25 scores in terms of ROUGE-1, respectively.

Comparison of Various Scaling Methods We have emphasized the importance of automatic coefficient learning in Section 3.2. The forward pass of RK2-block can be described as $y_{t+1} = y_t + \gamma_1 \cdot F_1 + \gamma_2 \cdot F_2$, where γ_1 and γ_2 are coefficients which can be numerical suggested or learnable. Here we exhibit the comparison of various scaling methods on the WMT'14 En-De dataset, and the results are listed in Table 10. We can see that RK2-block (learnable γ_i) equips with single sigmoid gate (line 5 in Table 10) yields best results on both shallow and deep configurations. The observation here reveals that appropriate scaling functions can further improve the RK2-block. Tanh activation even brings negative impacts on the performance, especially when the model is deep. A possible explanation is that Tanh produces a larger range ($[-1, 1]$) which is more difficult to optimize than the sigmoid function.

[11] BLEU+case.mixed+numrefs.1+smooth.exp+tok.13a+version.1.2.12

[12] We only compared models without using pre-training.

Model	ROUGE-1	ROUGE-2	ROUGE-L
LEAD3	40.24	17.70	36.45
NEUSUM (Zhou et al., 2018)	41.59	19.01	37.98
PGNet (See et al., 2017)	39.53	17.28	36.38
Soft Fusion (Liu et al., 2020b)	41.00	18.30	37.90
Bottom-Up Summarization (Gehrmann et al., 2018)	41.22	18.68	38.34
Residual-block	40.47	17.73	37.29
RK2-block	41.58	18.57	38.41
RK4-block	**41.83**	**18.84**	**38.68**

Table 9: ROUGE scores of various models on the CNN/DailyMail dataset.

Model	γ_1	γ_2	6-layer	24-layer
weight sharing	1	1	28.51	29.60
RK2-block	1/2	1/2	28.67	29.85
RK2-block ($\gamma_i = 1$)	1	1	28.77	30.01
RK2-block (learnable $\gamma_i = 1$)	scalar	scalar	28.80	30.13
RK2-block (learnable γ_i)	sigmoid	sigmoid	28.74	30.06
RK2-block (learnable γ_i)	sigmoid	(1 - sigmoid)	28.86	30.29
RK2-block (learnable γ_i)	tanh	tanh	28.45	29.47

Table 10: Comparison of various scaling functions on the WMT14' En-De dataset.

Case Study on the GEC Task Table 11 summarizes several cases from the GEC task. Here, we take a comparison between the baseline and the RK4-block due to its superiority on the GEC task. We can clearly see that the proposed RK4-block delivers more accurate corrections compared with the baseline when handling subject verb agreement (Case2), collocation (Case1, Case3), spelling (Case4) and other issues. More specifically, Figure 7 illustrates the statistics of different error type annotated by ERRANT (Bryant et al., 2017), a grammatical ERRor ANnotation Toolkit designed to automatically annotate parallel error correction data. More details please refer to Bryant et al. (2017)'s work. With the help of ERRANT, we can carry out a detailed error type analysis. As shown in Figure 7, RK4-block corrects the input in a more similar way with the reference, though there is still a large gap between them. Limited by the model ability, the baseline sometimes even cannot generate the right corrections, e.g. R:PUNCT and M:OTHER cases.

D Comparison with Related Work

As we aforementioned, the ODE design schema somehow shares a similar merit with the weight sharing, especially when the coefficients are set to 1. This is because we reuse the same function F to compute the intermediate approximation at each timestep, and it is also a effective way to apply the higher-order ODE into the Transformer architecture. Compared with weight sharing (line 1 in Table 10), ODE Transformer variants can deliver better performance within the same computation cost, demonstrating the effectiveness of ODE design schema.

Next, we make a detail comparison between the proposed ODE Transformer and previous studies (Baier-Reinio and De Sterck, 2020; Zhu and Fu, 2018; Zhang et al., 2021) to avoid the potential misunderstandings.

Compared with RKNet RKNet (Zhu and Fu, 2018) is mainly designed to improve the ResNet using implicit Runge-Kutta methods for vision tasks. There are some differences between ours and RKNet. (i) We mainly conduct experiments on sequence generation tasks, e.g. machine translation, abstract summarization, and grammar error correction tasks. They focused on the image classification task. (ii) Except for the integration of ODE into the Transformer design schema, we also make an analysis on how to choose appropriate coefficients

Case1	Source	What 's more , **various of** cultures can be shown to us through **social medias** .
	Reference	What 's more , **various** cultures can be shown to us through **social media** .
	Baseline	What 's more , **various** cultures can be shown to us through **social medias** .
	RK4	What 's more , **various** cultures can be shown to us through **social media** .
Case2	Source	Social media sites such as Facebook **has allow** us to share our pictures or even chat online with our parents while we are overseas .
	Reference	Social media sites such as Facebook **have allowed** us to share our pictures or even chat online with our parents while we are overseas .
	Baseline	Social media sites such as Facebook **allow** us to share our pictures or even chat online with our parents while we are overseas .
	RK4	Social media sites such as Facebook **have allowed** us to share our pictures or even chat online with our parents while we are overseas .
Case3	Source	**On one side** , it is **obviousaly** that many advantages have been brought to our lives .
	Reference	**On the one hand** , it is **obvious** that many advantages have been brought to our lives .
	Baseline	**On one hand** , it is **obvious** that many advantages have been brought to our lives .
	RK4	**On the one hand** , it is **obvious** that many advantages have been brought to our lives .
Case4	Source	Other than that , I believe that the **stong** bond we have with our family is the biggest pillar of support to the carrier .
	Reference	Other than that , I believe that the **strong** bond we have with our family is the biggest pillar of support to the carrier .
	Baseline	Other than that , I believe that the **stong** bond we have with our family is the biggest pillar of support to the carrier .
	RK4	Other than that , I believe that the **strong** bond we have with our family is the biggest pillar of support to the carrier .

Table 11: Several examples from the GEC task. Here, source and reference denote the model input and the correction result, respectively. **Green** words are good corrections, while **Red** words are bad corrections.

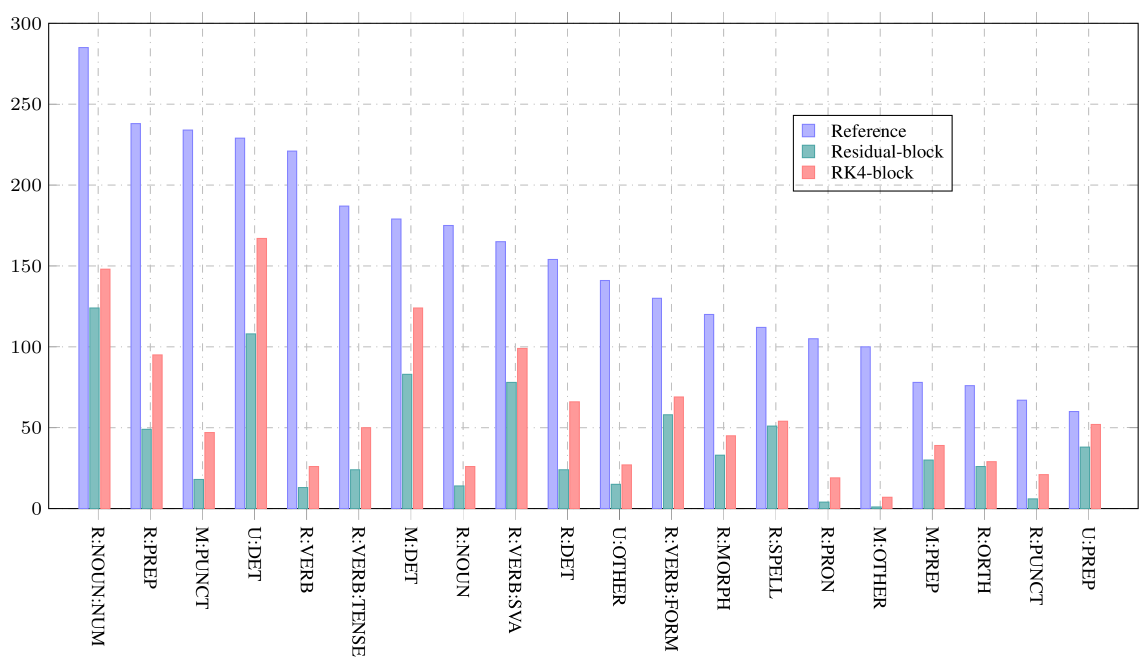

Figure 7: Statistics of different error type information.

of intermediate approximations. And we bridge the relationship between the ODE design schema with the explicit weight sharing. (iii) We also offer an automatically coefficient learning method for RK2-block which delivers the best performance in different configurations.

Compared with N-ODE As we discussed in the related work, our work is complementary to Baier-Reinio and De Sterck (2020)'s work, that we empirically demonstrate the effectiveness of integrating ODE design schema into Transformer on several sequence generation tasks. This work may shed light on the design of effective Transformer architectures from the numerical perspective and provides stronger baselines to the literature.

Compared with CSAODE The differences between these two work are summarized below: (i) As we emphasized above, the benchmarks we experimented on are quite different. They mainly validated the proposed CSAODE on text classification and QA tasks. (ii) The proposed CSAODE (Zhang et al., 2021) is an extension of neural ODE (cheng et al., 2018), the motivation is quite different. They aim to effectively calculate the contiguous states of hidden features only via one-layer parameters and proposed a self-attention solver to fix the issue. While our motivation is to employ higher-order ODE solutions to reduce the truncation errors produced by each layer. On the other hand, CSAODE is still a single-layer model, and ours is a multi-layer sequence-to-sequence model. We also show the comparison of different components based on higher-order ODE solutions (See Figure 4). (iii) Single-layer model is not strong enough to solve complicated tasks, e.g. machine translation. However, when stacking several layers, we need to re-consider the error accumulation among layers, that each layer is an individual ODE solver. How to mitigate the error accumulation is the main goal in this work, which is not discussed in their work.

E Derivations of the Equation

Let $\mathcal{E}$ be the loss of training, L be the number blocks of the model, and y_L be the model output. Here, we define

$$z_k = y_k + F(y_k, \theta_k) \tag{27}$$

Then the information flow of the RK2 method can be described as follows:

$$\begin{aligned} y_{k+1} &= y_k + \frac{1}{2}F(y_k, \theta_k) + \\ &\quad \frac{1}{2}F(y_k + F(y_k, \theta_k), \theta_k) \\ &= y_k + \frac{1}{2}F(y_k, \theta_k) + \frac{1}{2}F(z_k, \theta_k) \end{aligned} \tag{28}$$

where $\frac{\partial z_k}{\partial y_k} = 1 + \frac{\partial F(y_k,\theta_k)}{\partial y_k}$. In this way, the detail derivation of Eq. (28) is as follows:

$$\begin{aligned} \frac{\partial y_{k+1}}{\partial y_k} &= 1 + \frac{1}{2}\frac{\partial F(y_k, \theta_k)}{\partial y_k} + \frac{1}{2}\frac{\partial F(z_k, \theta_k)}{\partial z_k} \cdot \frac{\partial z_k}{\partial y_k} \\ &= \frac{1}{2} \cdot \Big(1 + 1 + \frac{\partial F(y_k, \theta_k)}{\partial y_k} + \frac{\partial F(z_k, \theta_k)}{\partial z_k} \cdot \\ &\quad \Big(1 + \frac{\partial F(y_k, \theta_k)}{\partial y_k}\Big)\Big) \\ &= \frac{1}{2} \cdot \Big(1 + \Big(1 + \frac{\partial F(z_k, \theta_k)}{\partial z_k}\Big) \cdot \\ &\quad \Big(1 + \frac{\partial F(y_k, \theta_k)}{\partial y_k}\Big)\Big) \end{aligned} \tag{29}$$

With the chain rule, the error $\mathcal{E}$ propagates from the top layer y_L to layer y_t by the following formula:

$$\frac{\partial \mathcal{E}}{\partial y_t} = \frac{\partial \mathcal{E}}{\partial y_L} \cdot \frac{\partial y_L}{\partial y_{L-1}} \cdot \frac{\partial y_{L-1}}{\partial y_{L-2}} \cdots \frac{\partial y_{t+1}}{\partial y_t} \tag{30}$$

Here we have

$$g_k = \Big(1 + \frac{\partial F(y_k, \theta_k)}{\partial y_k}\Big) \cdot \Big(1 + \frac{\partial F(z_k, \theta_k)}{\partial z_k}\Big)$$

Then, put the Eq. (30) into Eq. (29), the gradient of $\mathcal{E}$ at y_t is

$$\frac{\partial \mathcal{E}}{\partial y_t} = \frac{\partial \mathcal{E}}{\partial y_L} \cdot \frac{1}{2^{L-t}} \cdot \prod_{k=t}^{L-1}(1 + g_k) \tag{31}$$

Similarly, we can easily obtain the gradient of RK2 method where $\gamma_i = 1$:

$$\begin{aligned} \frac{\partial \mathcal{E}}{\partial y_t} &= \frac{\partial \mathcal{E}}{\partial y_L} \cdot g_{L-1} \cdot g_{L-2} \cdots g_t \\ &= \frac{\partial \mathcal{E}}{\partial y_L} \cdot \prod_{k=t}^{L-1} g_k \end{aligned} \tag{32}$$